Consequences of Single-Site Mutations in the Intestinal Fatty Acid Binding Protein†

Masoumeh Rajabzadeh,‡ Jeff Kao,§ and Carl Frieden*,||

Department of Biochemistry and Molecular Biophysics, Washington University School of Medicine, St. Louis, Missouri 63110, Department of Chemistry, Washington University School of Medicine, St. Louis, Missouri 63130, and Ciphergen Biosystems, Inc., Fremont, California 94555

Received July 11, 2003; Revised Manuscript Received August 26, 2003

ABSTRACT: The intestinal fatty acid binding protein (IFABP) is a small (15 kDa) protein consisting mostly of 10 antiparallel β-strands (A−J) and a small helical region that serves as a portal for the ligand. Two β-sheet structures (strands A−E and F−J) surround a cavity into which the ligand binds. In this work, we investigated how changes in the side chains of specific residues are propagated through the structure. To determine what these changes were and how they relate to changes in stability, ^{15}N chemical shift perturbations were measured and compared to those of the wild-type protein. Seven mutations, five of which change either valine or leucine to glycine, have been examined. All these mutants were less stable than wild-type IFABP, suggesting some structural changes. For five of the mutants, the data suggest that destabilization of a small region of the protein propagates throughout the structure, resulting in an overall decrease in stability. In two (Leu38Gly and Leu89Gly), the loss of cooperativity in the equilibrium denaturation curves suggests that the destabilization of one region may not be transmitted to other regions in a cooperative manner. It is shown that the effect of mutating hydrophobic residues is much greater than that observed upon mutation of a solvent-exposed polar residue.

The rat intestinal fatty acid binding protein (IFABP,[1] PDB entry 1IFB) is a small (15 kDa) protein consisting primarily of antiparallel β-strands surrounding a large interior cavity into which ligand binds. There is a small helical region that is believed to serve as the portal for ligand binding. The structure of IFABP, one of a large class of proteins that are similar in structure, has been determined both by X-ray crystallography (*1*−*3*) and by NMR (*4*−*7*). One turn between two antiparallel β-strands, called the D−E turn, is unusual because of a relatively large gap between adjacent strands but no hydrogen bonds between the backbone atoms. Previous studies have shown that a leucine residue (Leu64) in the D−E turn is essential for stabilizing the final folded form of the protein, and it was proposed that this residue could play a role in both the early (hydrophobic collapse) and late (structure stabilization) steps in the folding process (*8*).

Site-directed mutagenesis is a common technique for establishing the importance of specific residues in protein function. What is usually ignored is whether the mutation of a single residue in a protein can affect regions that are distant from the site of the mutation. To show how mutation of a single residue is propagated throughout the molecule,

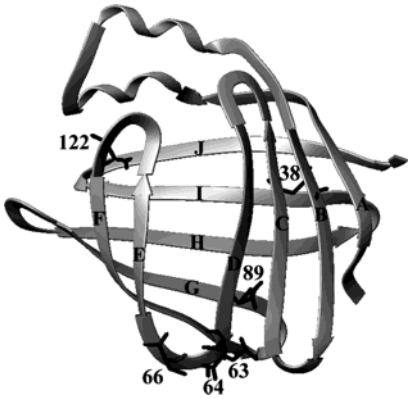

FIGURE 1: X-ray crystal structure of the intestinal fatty acid binding protein (*33*). Positions and numbering of the residues that have been mutated are shown. The ribbon diagram was made using Molmol (*34*).

^{15}N chemical shifts of individual residues of single-site mutants (Figure 1) were recorded and compared to their respective values in wild-type IFABP by using two-dimensional ^{1}H−^{15}N heteronuclear single-quantum coherence (HSQC) NMR spectra. The residues chosen were mostly hydrophobic since they were believed to be important in the folding process on the basis of earlier data (*8*−*13*). Mutations of these residues decreased the stability of the protein in all cases. In those cases where there was a loss in cooperativity upon denaturation, we interpreted the data to mean that destabilizing one region of the protein had minimal effects on the stability of other regions.

Chemical shifts have been used in ligand binding studies for FK506 binding protein and stromelysin (*14*−*16*), monitoring changes in protein backbone structure of histidine-

† This work was supported in part by NIH Grant DK13332.

* To whom correspondence should be addressed. Phone: (314) 362-3344. Fax: (314) 362-7183. E-mail: frieden@biochem.wustl.edu.

‡ Ciphergen Biosystems, Inc.

§ Department of Chemistry, Washington University School of Medicine.

|| Department of Biochemistry and Molecular Biophysics, Washington University School of Medicine.

[1] Abbreviations: IFABP, intestinal fatty acid binding protein; HSQC, heteronuclear single-quantum coherence; CD, circular dichroism; TB, terrific broth.

10.1021/bi0301688 CCC: $25.00
Published on Web 09/26/2003

containing protein (HPr) from *Staphylococcus carnosus*, basic pancreatic trypsin inhibitor (BPTI), and hen lysozyme under pressure (*17*−*19*), and mapping of intermolecular surfaces of turkey ovomucoid third domain (OMTKY3) with bovine chymotrypsin A_α and matrix metalloproteinase (MMP) on the N-terminal domain of the tissue inhibitor of metalloproteinase-2 (N-TIMP-2) (*20*, *21*).

MATERIALS AND METHODS

Mutagenesis, Protein Expression, and Purification. Mutagenic primers were obtained from Integrated DNA Technologies (Coralville, IA). The QuikChange site-directed mutagenesis kit was obtained from Stratagene (La Jolla, CA).

Mutations were introduced into the expression vector pMON5840−IFABP recombinant plasmid using site-directed mutagenesis. The mutant plasmids were then identified by sequencing.

Escherichia coli strain MG1655, transformed with a mutated pMONIFABP construct, was incubated in 10 mL of TB medium containing 100 μg/mL ampicillin for approximately 7 h and 5 mL transferred to 250 mL of minimal medium containing [98%-^{15}N]ammonium chloride (Cambridge Isotope Laboratories) in a 500 mL flask for overnight incubation. Seven hundred milliliters of minimal medium in a 1 L flask was inoculated from this stock to give an OD_{600} of 0.26. Protein expression was induced by the addition of 7 mL of nalidixic acid (10 mg/ml) at an OD_{600} of 2−2.5, and the cells were grown to an OD_{600} of 4, harvested, and frozen at −70 °C.

All the IFABP mutants except Val66Gly were recovered from inclusion bodies and were purified following the previously published procedure (*12*), except that the final Sephadex G50 column step was not used.

NMR Spectroscopy. Measurements were performed at 22 °C on a Varian Unity 600 MHz spectrometer equipped with a Nalorac triple-resonance gradient probe. Mutants Leu38Gly and Leu64Ala were run on a Varian Inova 600 MHz spectrometer with a Varian 5 mm triple-axis gradient probe. Two-dimensional ^{1}H−^{15}N HSQC spectra were collected with spectral widths of 4.5 and 9.2 kHz and 1024 and 2048 complex points along the F_1 (^{15}N) and F_2 (^{1}H) frequency dimensions, respectively, using the gradient- and sensitivity-enhanced pulse sequence of Kay and co-workers (*22*). NMR samples (600 μL) were prepared, and contained ∼1 mM [^{15}N]IFABP mutant, 20 mM potassium phosphate buffer (pH 6.3), 0.05% NaN_3, and 10% D_2O.

The NMR probe was tuned and matched; the magnetic field was shimmed, and the 90° pulse widths were optimized for each sample. A ^{1}H−^{15}N HSQC spectrum was recorded for each sample with a total experimental time of approximately 390 min. The two-dimensional (three-dimensional) data were processed using the Varian VNMR software package. Data were linear predicted to 512 complex points in the t_1 dimension and then zero-filled to give 2048 and 1024 total points in the F_2 and F_1 dimensions, respectively. Spectra were apodized with appropriate window functions to give the desired resolution enhancement. ^{1}H chemical shifts were referenced versus sodium 3-(trimethylsilyl)-propionic acid-2,2,3,3-d_4 (TSP), and ^{15}N chemical shifts were indirectly referenced to liquid NH_3 using ammonium chloride. Processed spectra were imported for display and analysis into Sparky (T. D. Goddard and D. G. Kneller, *SPARKY*, version 3.01, University of California, San Francisco, CA).

All the mutants were characterized in a residue-specific manner by collection of two-dimensional ^{1}H−^{15}N HSQC NMR experiments. The nitrogen chemical shift perturbations were detected by comparing the ^{15}N chemical shifts of the residues in the ^{15}N-labeled mutants with the ^{15}N chemical shifts of the wild-type residues. Ambiguities in the assignment of some of the unknown resonances were eliminated by inspection of three-dimensional ^{1}H−^{15}N TOCSY-HSQC spectra for several mutants (Leu64Ala, Leu64Gly, Val66Gly, Leu89Gly, and Val122Gly). Again, gradient- and sensitivity-enhanced pulse sequences of Kay and co-workers were utilized (*22*, *23*). Experimental parameters were the same as the analogous parameters described above in detail for ^{1}H−^{15}N HSQC spectroscopy.

Fluorescence Measurements. Fluorescence data were obtained using a PTI Alphascan fluorometer (Photon Technology International, South Brunswick, NJ) with an excitation wavelength of 290 nm and an emission wavelength of 327 nm. A buffer blank spectrum was always subtracted from the protein spectrum. Denaturation curves were obtained using a protein concentration of 1−2 μM as a function of urea concentration. Experiments were performed in 0.02 M potassium phosphate buffer and 0.05% sodium azide at pH 6.3 and 20 °C.

Circular Dichroism Measurements. All experiments were performed on a Jasco J-715 spectropolarimeter. For data in the far-UV region (190−250 nm), spectra were obtained using a 0.02 cm light path. The protein concentration was 0.5 mg/mL. For data in the near-UV region (250−310 nm), the protein concentration was also 0.5 mg/mL using a 1 cm light path. All data were obtained using 0.02 M potassium phosphate buffer (pH 6.3) containing 0.05% sodium azide at room temperature.

Refolding Kinetics. The kinetics of refolding were followed using an Applied Photophysics stopped-flow spectrophotometer (model SX18MV) interfaced with an Archimedes computer. Changes in fluorescence (λ_{ex} = 290 nm and λ_{em} > 305 nm with a WG305 Schott glass cutoff filter) were followed at 20 °C. The unfolded proteins were preincubated in buffered urea (6 M), 0.02 M potassium phosphate (pH 6.3), and 0.05% NaN_3 and diluted 6-fold using a syringe ratio of 5:1. The final protein concentration was 2.0 μM (0.03 μg/μL).

RESULTS

Rationale for Choosing Specific Residues. The rationale for these mutations was to explore how altering the side chains of specific residues would affect spatially distant regions and how these changes might relate to protein stability. Some of the specific residues that were chosen were those suggested from previous experimental data to be important in the folding process (*8*−*13*). For each mutant, the residue was replaced with glycine to remove all side chain interactions even though it was recognized that glycine could lead to more drastic changes than other amino acids. In addition, one residue, Leu64, was replaced with alanine for comparison to the glycine mutation.

The D−*E Turn.* Of the four residues in the D−E turn (Glu, Leu, Gly, and Val), the crystal structure suggests that the

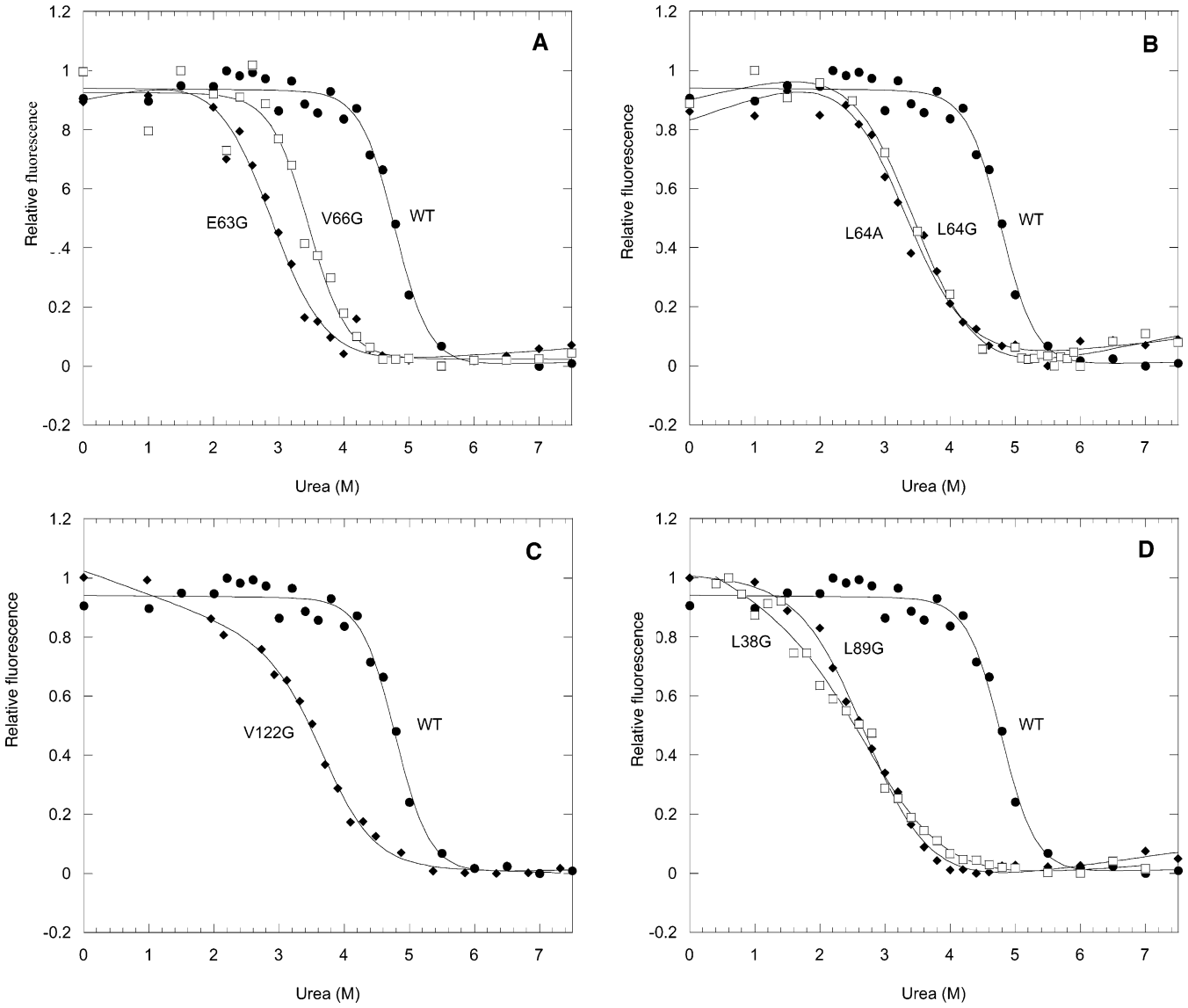

FIGURE 2: Denaturation of the apo wild type and mutants of IFABP as measured by changes in the intrinsic fluorescence (λ_{ex} = 290 nm, λ_{em} = 327 nm) as a function of urea concentration. Experiments were performed in 20 mM potassium phosphate buffer and 0.05% NaN_3 at pH 6.3 and 20 °C. The protein concentrations were 1−2 μM. The fluorescence intensity at 327 nm was normalized to a maximum value of 1.0. The solid lines through the data are fits to data assuming a two-state unfolding transition. (A) Unfolding transition of apo wild-type, Glu63Gly, and Val66Gly IFABP. (B) Unfolding transition of apo wild-type, Leu64Gly, and Leu64Ala IFABP. (C) Unfolding transition of apo wild-type and Val122Gly IFABP. (D) Unfolding transition of apo wild-type, Leu38Gly, and Leu89Gly IFABP.

side chain of Leu64 makes numerous contacts with residues in other strands while Val66 and Glu63 are solvent-exposed. Therefore, mutations of these latter two residues might not be expected to change the structure drastically. As shown in Figure 2A, these two mutants, while less stable than the wild type, show a degree of cooperativity in urea-induced unfolding similar to that of the wild type. There were, however, differences in the effect of the mutations, and these will be discussed later.

Previous investigations have shown the D−E turn to be important in the folding and stability of IFABP (*8*) and specifically that Leu64 may be involved in an initial collapse of hydrophobic residues. Even though IFABP does not have a large tightly packed hydrophobic core, it is believed that the collapse occurs around residues (Phe47, Phe62, Leu64, Phe68, Trp82, Met84, and Leu89) from different strands (C−E and G), all of which are hydrophobic (*8*, *24*). It was also shown that mutants lacking Leu64 were all less stable than the wild-type protein, and it was concluded that the decreased stability arose from the loss of interactions of the leucine side chain with side chains in neighboring strands (*8*).

To investigate the role of the side chain, we have substituted alanine as well as glycine in position 64. While both mutants (Leu64Gly and Leu64Ala) are similar in stability to each other, they are both less stable than the wild type (Figure 2B). The difference in chemical shift perturbations between these two mutants, as can be seen in Figures 5B and 6B, will be discussed later.

The I−J Turn. Studies by Hodsdon and Frieden have shown that the region around Gly121, the turn between the last two β-strands, persists at high denaturant concentrations (*10*). Moreover, studies on the turns in IFABP have shown that the mutant Gly121Val folds much slower than the wild-type protein (*9*, *12*). Therefore, this region of the protein (Val122Gly) was a candidate for investigation. Figure 2C

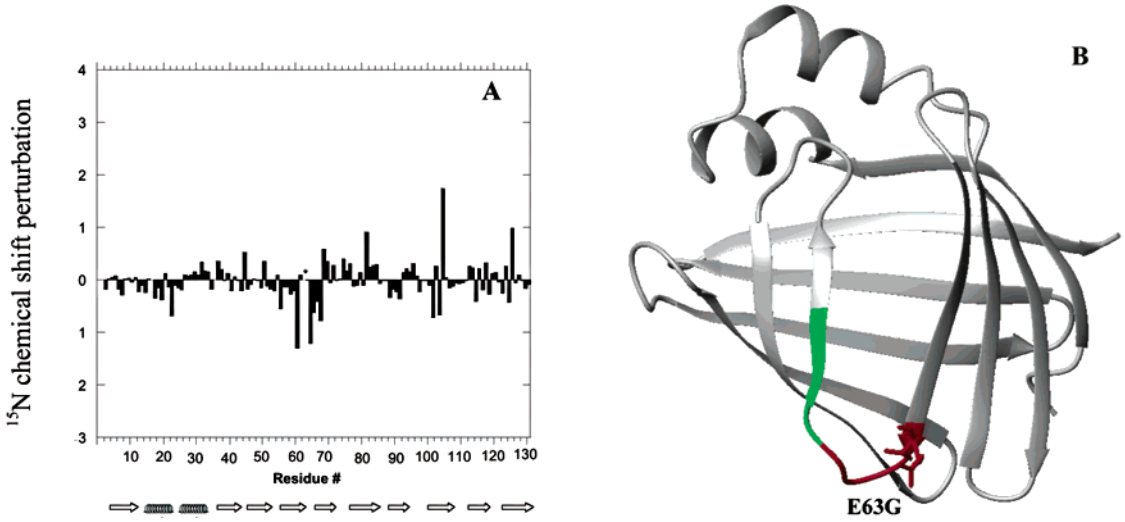

FIGURE 3: (A) Amide nitrogen chemical shift changes determined as the difference between the wild type and Glu63Gly, plotted as a function of amino acid residue number. One standard deviation from the mean is 0.26 ppm for this histogram. The asterisk denotes a residue that could not be assigned. (B) Molmol (*34*) structure of IFABP with portions of the Glu63Gly mutant that show chemical shift perturbation changes relative to the wild type. Red denotes amino acids that are within 4 Å of the mutation site, while green denotes amino acids more than 4 Å from the site of the mutation.

shows considerable loss of cooperativity in the equilibrium denaturation curve compared to the wild type.

Leu89 and Leu38. Earlier work by Jiang and Frieden had shown that the protein with a Leu89 mutation was less stable than the wild type (*11*), and it was concluded that this region of the protein was highly protected from solvent and was important for the final stability of the protein. In addition, it is also one of the residues that plays a role in the collapse of residues with hydrophobic side chains mentioned earlier. As shown in Figure 2D, Leu89Gly, like Leu38Gly **(**also shown in Figure 2D), was the least stable mutant and exhibited weak cooperativity in the equilibrium unfolding curve relative to the wild-type protein.

Leu38 was chosen because it has contacts with other nearby hydrophobic residues (hydrophobic residues close to this residue are Trp6, Leu36, Ile40, Val49, Leu113, and Phe128) to examine the role of this hydrophobic cluster in the structure of IFABP. It was not only unstable, showing a loss of cooperativity in the denaturation curve, but also prone to aggregation. The maximum wavelength for this mutant was 320 nm, instead of 327 nm as seen for the other mutants which suggests that the tryptophans in this mutant are more buried than in the other mutants. In contrast to all other mutants, the far-UV CD of this mutant could not be superimposed on that of the wild type. This may be due to the presence of the denatured protein, since the HSQC spectrum of this mutation also shows peaks where the denatured peaks occur for wild-type IFABP.

The equilibrium denaturation data shown in Figure 2 were analyzed using the equation assuming a two-state process (*25*). Examination of some of these curves, however, shows so much loss of cooperativity that such an analysis is not appropriate for determining m or $\Delta G°$ values.

The far-UV CD spectra (from 190 to 250 nm) of all mutants except Leu38Gly (as noted above) can be superimposed with that of the wild type. However, there are some differences in the near-UV CD spectra (from 250 to 310 nm) of all the mutants, indicating differences in local and/or tertiary interactions (data not shown). This may be related to different interactions of the mutated sites with phenylalanines, tryptophans, and tyrosines on neighboring strands.

Chemical Shift Perturbations. The nitrogen chemical shift changes of the residues in each mutant are depicted in bar graphs, and the effect of the mutation on the structure is shown in Figures 3−9. For all the mutants that were studied, we assumed that values of the chemical shift perturbation more than one standard deviation from the mean for at least three consecutive residues reflect regions in which there is either some sort of local rearrangement or some alteration in electronic shielding. Residues that could not be assigned are denoted with asteriska in the bar graphs. Each structure shows two colors. Those regions colored red are within 4 Å of the side chain that has been replaced. Those regions colored green are more than 4 Å from the site of the mutation and presumably represent distant perturbations as a result of the mutation.

Figures 3 and 4 show results for mutants Glu63Gly and Val66Gly, respectively. From the crystal structure, the side chains of both these residues are solvent-exposed. As shown in Figure 4B for the Val66Gly mutant, however, the Val60−Leu72 region has been more affected by the mutation. The results suggest the hydrophobic valine side chain, while still solvent-exposed, may be more buried than indicated by the X-ray structure.

It is of particular interest to compare mutants Leu64Ala and Leu64Gly (Figures 5 and 6, respectively) since the results are similar but not identical. In Leu64Ala, residues that are affected correspond to strands C, D, and F in the protein as shown in Figure 5B. This change has propagated to strands H and I as well. Figure 6A shows the regions affected in Leu64Gly which correspond to strands C, D, F, and G as shown by the structure. Strand E is not affected much in Leu64Gly, which is to be expected as it is not hydrogen bonded to strand D. Residues L102−V105 also exhibit chemical shift changes in the Leu64Gly mutant. Since these residues have not been confirmed in the three-dimensional TOCSY-HSQC spectrum, however, the assignments are not reliable.

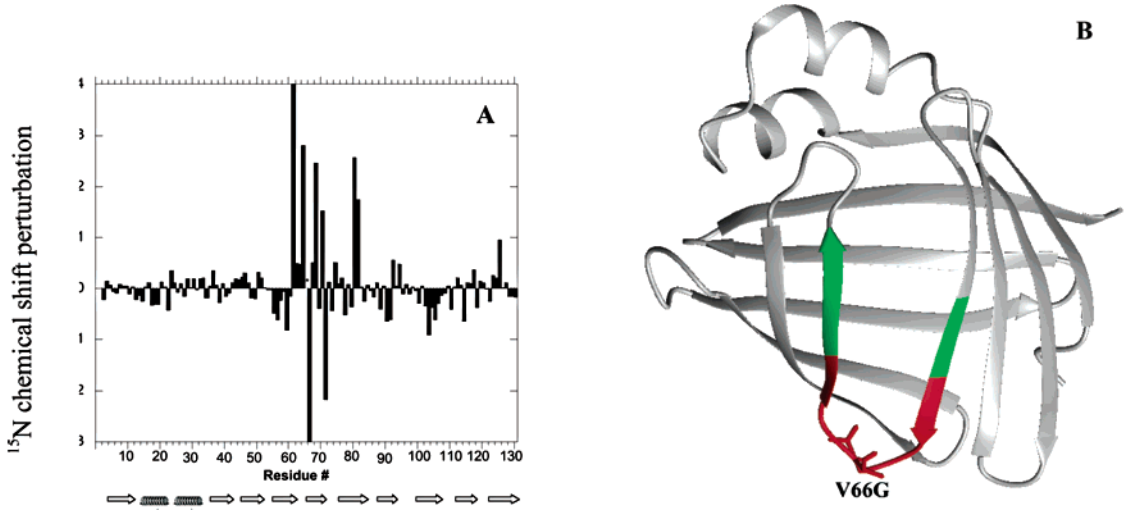

FIGURE 4: (A) Amide nitrogen chemical shift changes determined as the difference between the wild type and Val66Gly, plotted as a function of amino acid residue number. One standard deviation from the mean is 0.71 ppm for this histogram. The asterisk denotes a residue that could not be assigned. (B) Molmol (*34*) structure of IFABP with portions of the Val66Gly mutant that show chemical shift perturbation changes relative to the wild type. Red denotes amino acids that are within 4 Å of the mutation site, while green denotes amino acids morethan 4 Å from the site of the mutation.

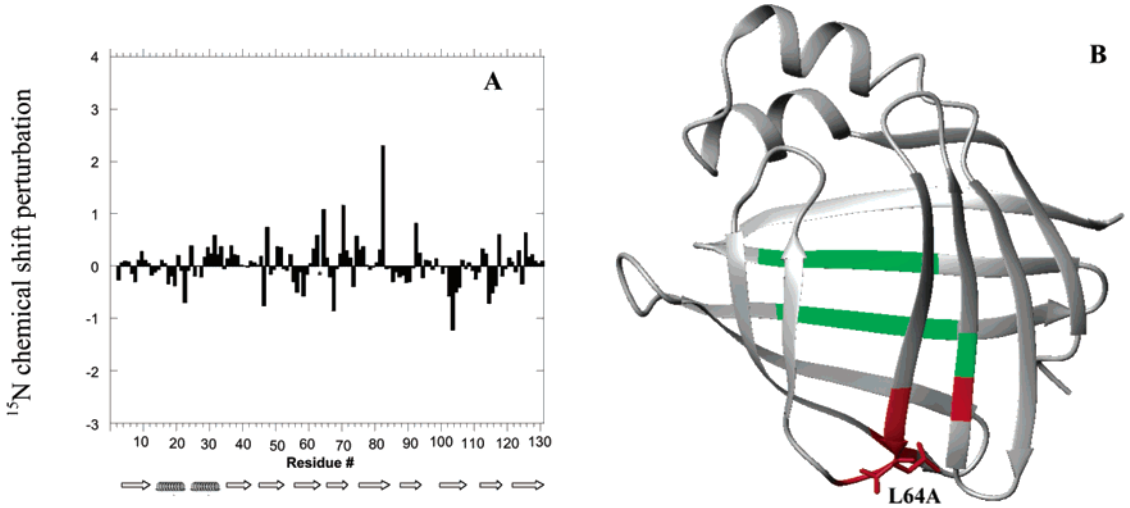

FIGURE 5: (A) Amide nitrogen chemical shift changes determined as the difference between the wild type and Leu64Ala, plotted as a function of amino acid residue number. One standard deviation from the mean is 0.40 ppm for this histogram. The asterisk denotes a residue that could not be assigned. (B) Molmol (*34*) structure of IFABP with portions of the Leu64Ala mutant that show chemical shift perturbation changes relative to the wild type. Red denotes amino acids that are within 4 Å of the mutation site, while green denotes amino acids more than 4 Å from the site of the mutation.

The results for Leu64Ala and Leu64Gly (Figures 5 and 6, respectively) differ. The difference could be a consequence of the larger size of the alanine side chain or to restriction of the ϕ and ψ angles of alanine relative to glycine.

The data for Val122Gly are shown in Figure 7. This mutation gave rise to some of the largest chemical shift changes of all the mutants. These changes are clustered around the first helical region of Phe17−Asn24, the last two strands (I and J), and the E−F turn. The helical region and the I and J strands have some residues that are close to the position that has been mutated, but the changes extend well beyond those regions. The data for Leu89Gly are shown in Figure 8.

Figure 9 shows the results for Leu38Gly. The β-strand (strand B) around Leu38 (residues 30−40) is affected the most, while there are smaller chemical shift perturbations in regions further away (residues 6−9 in the A strand and residues 50−52 and 104−107 in strands C and H, respectively). As mentioned earlier, this mutant was the most difficult with which to work and all the residues in the ^{15}N HSQC spectrum could not be assigned. Peaks that were not assigned included several around the mutation (His33, Asp34, Asn35, Lys37, Gly38, and Ile40).

DISCUSSION

Chemical Shift Perturbations. The following factors are said to contribute to ^{15}N shielding: backbone dihedral angles of neighboring residues (ψ_i and ϕ_{i-1}), the nature and conformation of the alkyl substituents of the immediately preceding residue, the side chain conformation of the residue, the effects of hydrogen bonding to ^{15}N, and the effects of longer-range electrostatic fields (*26*, *27*).

It has been shown that ^{15}N shifts are sensitive to hydrogen bonding [upfield for long hydrogen bonds and downfield for short hydrogen bonds (*26*)] since shorter hydrogen bonds (shorter H···O distance) cause a stronger polarization of the

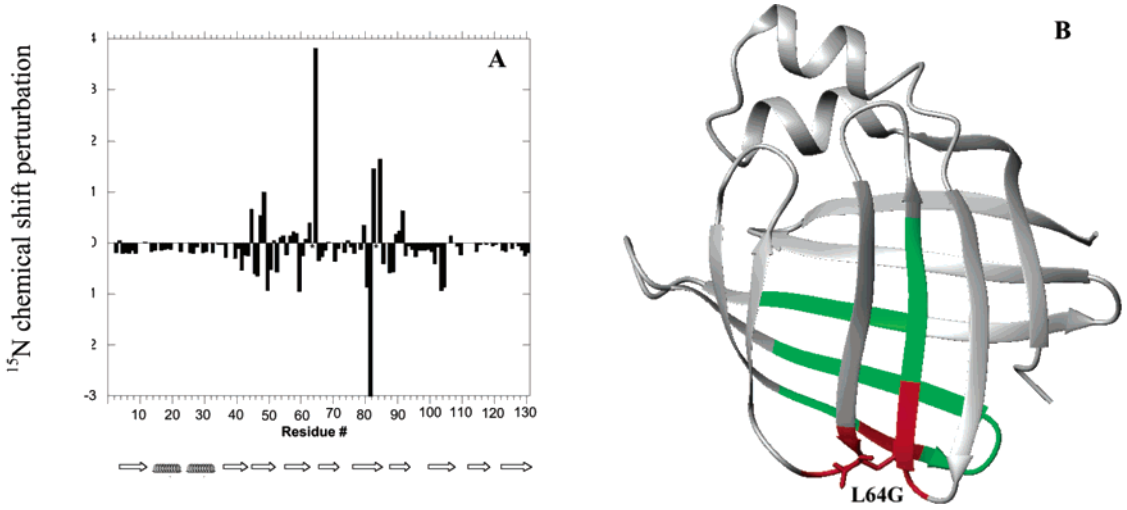

FIGURE 6: (A) Amide nitrogen chemical shift changes determined as the difference between the wild type and Leu64Gly, plotted as a function of amino acid residue number. One standard deviation from the mean is 0.51 ppm for this histogram. Asterisks denote residues that could not be assigned. (B) Molmol (*34*) structure of IFABP with portions of the Leu64Gly mutant that show chemical shift perturbation changes relative to the wild type. Red denotes amino acids that are within 4 Å of the mutation site, while green denotes amino acids more than 4 Å from the site of the mutation.

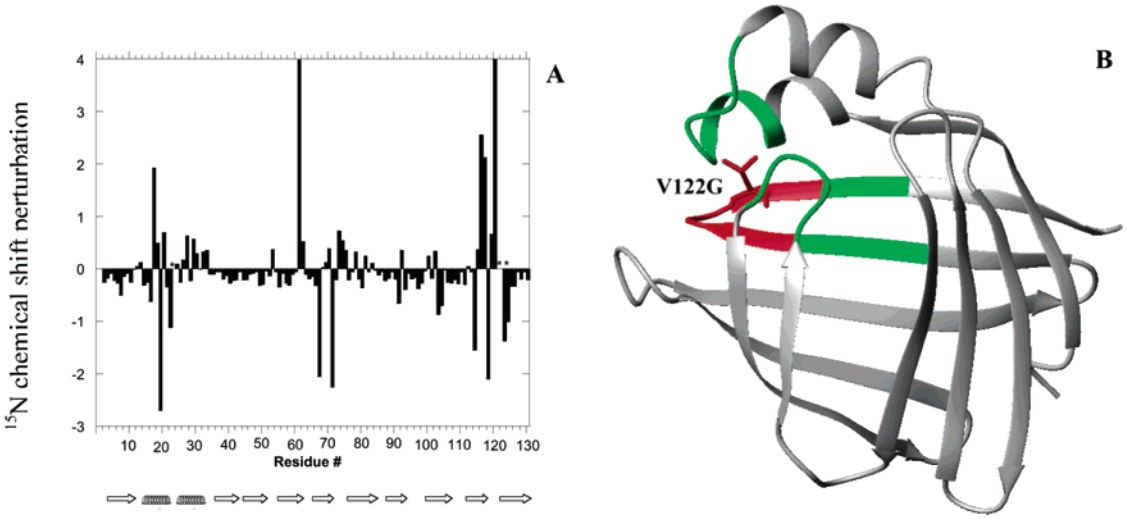

FIGURE 7: (A) Amide nitrogen chemical shift changes determined as the difference between the wild type and Val122Gly, plotted as a function of amino acid residue number. One standard deviation from the mean is 0.69 ppm for this histogram. Asterisks denote residues that could not be assigned. (B) Molmol (*34*) structure of IFABP with portions of the Val122Gly mutant that show chemical shift perturbation changes relative to the wild type. Red denotes amino acids that are within 4 Å of the mutation site, while green denotes amino acids more than 4 Å from the site of the mutation.

hydrogen bond. Hence, there is less shielding of the magnetic field, leading to a lower-field shift (higher parts per million, more deshielded, and positive bars), while larger hydrogen bond lengths are correlated with shifts to higher fields (lower parts per million, shielded, and negative bars). Even though ^{15}N chemical shifts have been analyzed, there has not been much progress in this area, and thus, their quantitative use has been hindered (*28*, *29*). For the two mutants which are solvent-exposed in the crystal structure (Glu63 and Val66), the only regions in which there are chemical shifts are those which are reasonably close in sequence to the site of the mutation. The mutations, however, in these cases are not totally benign. The mutant that would be expected to be the least perturbing based on solvent exposure and a slight effect on stability is Glu63. Even in this case, however, some structural changes appear in the D−E turn and the E strand (residues 64−69). Similarly for Val66, also solvent-exposed, the affected regions are those mostly in the D−E strands and the D−E turn.

The picture is quite different for those mutants in which the residue in the wild-type protein is more buried in the structure (Leu38, Leu64, Leu89, and Val122). Not only are these mutants less stable than the wild type, but the denaturation curve also appears to be less cooperative, indicating the presence of intermediates in equilibrium with either the folded or unfolded form. As noted above, the largest chemical shift perturbations are observed for the Val122Gly mutant. Val122 is located in strand J and has two hydrogen bonds with Tyr119 in strand I. Therefore, it is not surprising that these are the two strands that have been perturbed the most. As can be seen in Figure 7B, this mutation has affected an entirely different portion of the molecule compared to mutations close to the D−E strand. It should be remembered that mutation of Gly121 to valine

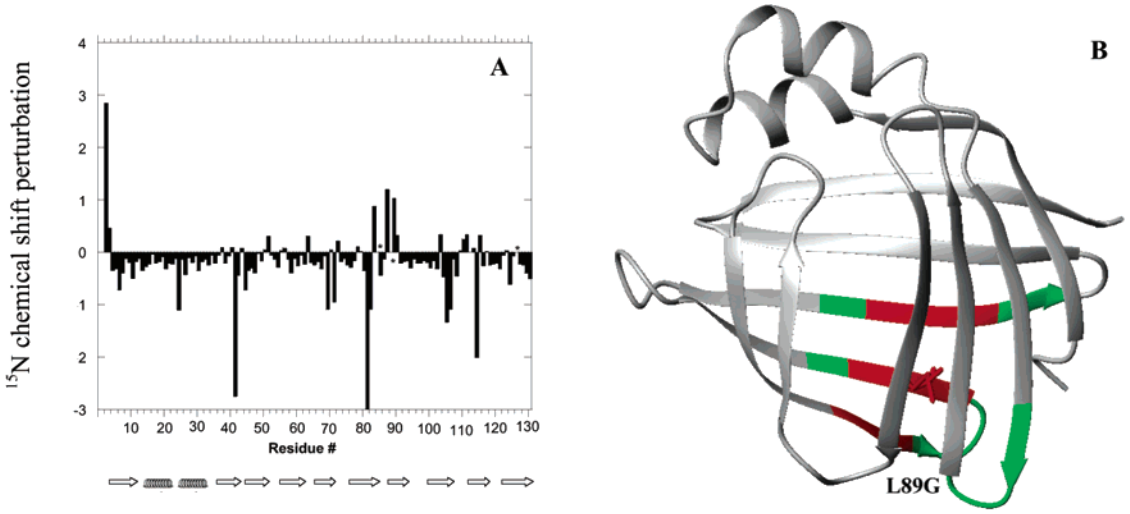

FIGURE 8: (A) Amide nitrogen chemical shift changes determined as the difference between the wild type and Leu89Gly, plotted as a function of amino acid residue number. One standard deviation from the mean is 0.50 ppm for this histogram. Asterisks denote residues that could not be assigned. (B) Molmol (*34*) structure of IFABP with portions of the Leu89Gly mutant that show chemical shift perturbation changes relative to the wild type. Red denotes amino acids that are within 4 Å of the mutation site, while green denotes amino acids more than 4 Å from the site of the mutation.

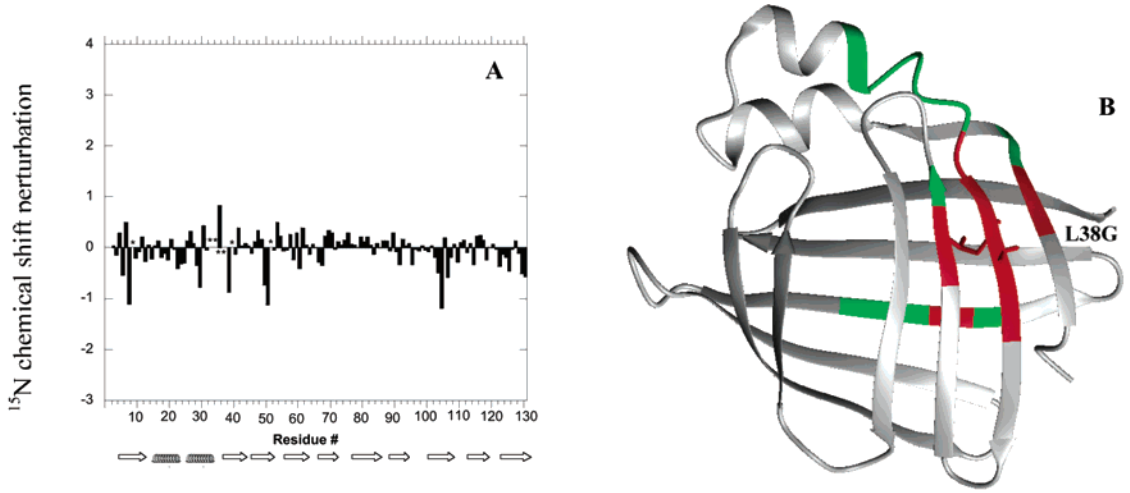

FIGURE 9: (A) Amide nitrogen chemical shift changes determined as the difference between the wild type and Leu38Gly, plotted as a function of amino acid residue number. One standard deviation from the mean is 0.23 ppm for this histogram. Asterisks denote residues that could not be assigned. (B) Molmol (*34*) structure of IFABP with portions of the Leu38Gly mutant that show chemical shift perturbation changes relative to the wild type. Red denotes amino acids that are within 4 Å of the mutation site, while green denotes amino acids more than 4 Å from the site of the mutation.

results in a dramatic reduction (up to at least 100-fold) of the folding rate (*12*) as does the Val122Gly change (data not shown). The region around this turn also appears to persist at high denaturant concentrations (*10*).

Another factor to take into account is the chemical shift of residues that are hydrogen bonded to the mutation site in the wild type. In all the mutants, the mutated residue has one or two hydrogen bonds to one or two other residues in the wild type. As shown in Table 1, there is a considerable chemical shift perturbation in the residues which have hydrogen bonds to the mutation site in the wild type in all cases except for one mutant (Leu64Ala).

Nevertheless, it must be mentioned that there is subjectivity in using ^{15}N chemical shifts to follow perturbations caused by single-site mutations. ^{15}N chemical shifts are very complex as they depend on many variables. As a consequence, instead of a single dominant factor there is a combination of effects that contributes to their chemical shift changes. Therefore, the interpretations of the shifts here are qualitative and used indirectly for structural information as well as for confirmation and validation of what is believed to be taking place.

Table 1: Nitrogen Chemical Shifts of Residues with Hydrogen Bonds to Mutation Sites in Wild-Type IFABP

mutation	hydrogen bond	distance from mutation (Å)	^{15}N shift (ppm)
Glu63Gly	Gly65	4	−1.2
	Val66	3	−0.62
Val66Gly	Glu63	3	0.50
	Trp82	5	1.73
Leu64Gly	Asn45	4	0.66
Leu64Ala	Asn45	4	0.03
Val122Gly	Tyr119*	3	−2.1
Leu89Gly	Arg106	3	−1.33
Leu38Gly	Trp6*	3	−0.55

Full use of experimentally determined chemical shift values will only be possible when an accurate method for

predicting how chemical shifts depend on the overall structure of the protein is available.

Stability and Chemical Shift Perturbations. One rationale for this study was to see whether there was any correlation between the stability of the protein and disruption of specific regions of the protein as measured by chemical shift perturbations. Examination of the equilibrium unfolding curves reveals some interesting points. Analysis of these curves includes determination of the degree of cooperativity of the unfolding transition. Thus, while all the mutants are less stable than the wild type, at least two (Leu38Gly and Leu89Gly) show a marked loss of cooperativity. Additionally, for Leu38Gly, the far-UV CD cannot be superimposed with that of the wild type or any of the other mutants. In this case, it would appear that this region close to the mutation remains unfolded and that there is a relatively high concentration of some folding intermediate.

In interpreting these results, we relate overall the chemical shift perturbations to the change in the overall stability of the protein. There are of course many factors that control protein stability. We have shown elsewhere (*30*−*32*) that side chain stabilization appears to occur coincident with overall stability and that side chain stabilization is a late, if not the last, step in the folding (*30*−*32*). Chemical shift perturbations of the type measured here, however, are not directly related to side chain stabilization but rather to changes in the hydrogen bonding network of the protein. It can be concluded that changes in hydrogen bonding can result from structural perturbations caused by the single-site mutations, especially since hydrogen bonds in β-strands are shorter than in helices. The differences in the degree of cooperativity of urea-induced denaturation suggest which regions of the protein may be important folding nuclei. Thus, disruptions of the structure caused by the Leu38Gly and Leu89Gly mutations lead to noncooperative unfolding transitions, suggesting that these regions can be disrupted without simultaneous disruption of the remaining structure. Common to both these mutations are portions of the B and H strands. We propose that these are not critical folding regions. In contrast, mutations at positions 63−66 and 122 still retain some higher degree of cooperativity in the unfolding transition. Thus, we propose that these regions are critical in the folding and stabilization process. This is consistent with earlier data showing that regions near Leu64 and Gly121 retain residual structure at high denaturant concentrations (*10*) and therefore may serve as nucleation sites for the folding process.

CONCLUSIONS

Several different mutations of the intestinal fatty acid binding protein have been introduced. Those in which the side chains are partially or fully solvent-exposed appear to be the least perturbing, but even in these mutants, the effect of the mutation is felt well beyond the locale of the side chain as measured by chemical shift perturbations. For mutations of residues that are not solvent-exposed, there are differing effects on the dependence of unfolding on urea concentration. Even those mutations which do not affect the cooperativity of the urea-induced denaturation curve make the protein less stable than the wild-type protein, suggesting that these mutations propagate changes cooperatively throughout the whole protein. In contrast, those mutants in which the urea-induced cooperativity of unfolding is low, changes are not propagated cooperatively.

ACKNOWLEDGMENT

We are indebted to Dr. Michael Hodsdon and Dr. David Cistola for valuable discussions regarding the interpretation of the NMR data.

REFERENCES

1. Scapin, G., Gordon, J. I., and Sacchettini, J. C. (1992) *J. Biol. Chem. 267*, 4253−4269.
2. Sacchettini, J. C., and Gordon, J. I. (1993) *J. Biol. Chem. 268*, 18399−18402.
3. Banaszak, L., Winter, N., Xu, Z., Bernlohr, D. A., Cowan, S., and Jones, T. A. (1994) *Adv. Protein Chem. 45*, 89−151.
4. Hodsdon, M. E., Ponder, J. W., and Cistola, D. P. (1996) *J. Mol. Biol. 264*, 585−602.
5. Hodsdon, M. E., and Cistola, D. P. (1997) *Biochemistry 36*, 1450−1460.
6. Hodsdon, M. E., and Cistola, D. P. (1997) *Biochemistry 36*, 2278−2290.
7. Zhang, F. L., Lucke, C., Baier, L. J., Sacchettini, J. C., and Hamilton, J. A. (1997) *J. Biomol. NMR 9*, 213−228.
8. Kim, K., Ramanathan, R., and Frieden, C. (1997) *Protein Sci. 6*, 364−372.
9. Chattopadhyay, K., Zhong, S., Yeh, S. R., Rousseau, D. L., and Frieden, C. (2002) *Biochemistry 41*, 4040−4047.
10. Hodsdon, M. E., and Frieden, C. (2001) *Biochemistry 40*, 732−742.
11. Jiang, N., and Frieden, C. (1993) *Biochemistry 32*, 11015−11021.
12. Kim, K., and Frieden, C. (1998) *Protein Sci. 7*, 1821−1828.
13. Ropson, I. J., and Frieden, C. (1992) *Proc. Natl. Acad. Sci. U.S.A. 89*, 7222−7226.
14. Shuker, S. B., Hajduk, P. J., Meadows, R. P., and Fesik, S. W. (1996) *Science 274*, 1531−1534.
15. Hajduk, P. J., Meadows, R. P., and Fesik, S. W. (1997) *Science 278*, 497−499.
16. Medek, A., Hajduk, P. J., Mack, J., and Fesik, S. W. (2000) *J. Am. Chem. Soc. 122*, 1241−1242.
17. Kalbitzer, H. R., Gorler, A., Li, H., Dubovskii, P. V., Hengstenberg, W., Kowolik, C., Yamada, H., and Akasaka, K. (2000) *Protein Sci. 9*, 693−703.
18. Akasaka, K., Li, H., Yamada, H., Li, R., Thoresen, T., and Woodward, C. K. (1999) *Protein Sci. 8*, 1946−1953.
19. Kamatari, Y. O., Yamada, H., Akasaka, K., Jones, J. A., Dobson, C. M., and Smith, L. J. (2001) *Eur. J. Biochem. 268*, 1782−1793.
20. Song, J., and Markley, J. L. (2001) *J. Mol. Recognit. 14*, 166−171.
21. Williamson, R. A., Carr, M. D., Frenkiel, T. A., Feeney, J., and Freedman, R. B. (1997) *Biochemistry 36*, 13882−13889.
22. Kay, L. E., Keifer, P., and Saarinen, T. (1992) *J. Am. Chem. Soc. 114*, 10663−10665.
23. Zhang, O., Kay, L. E., Olivier, J. P., and Forman-Kay, J. D. (1994) *J. Biomol. NMR 4*, 845−858.
24. Yeh, S. R., Ropson, I. J., and Rousseau, D. L. (2001) *Biochemistry 40*, 4205−4210.
25. Santoro, M. M., and Bolen, D. W. (1988) *Biochemistry 27*, 8063−8068.
26. Wishart, D. S., and Case, D. A. (2001) *Methods Enzymol. 338*, 3−34.
27. Le, H. B., and Oldfield, E. (1996) *J. Phys. Chem. 100*, 16423−16428.
28. McCoy, M. A., and Wyss, D. F. (2000) *J. Biomol. NMR 18*, 189−198.
29. Le, H. B., and Oldfield, E. (1994) *J. Biomol. NMR 4*, 341−348.
30. Bann, J. G., Pinkner, J., Hultgren, S. J., and Frieden, C. (2002) *Proc. Natl. Acad. Sci. U.S.A. 99*, 709−714.
31. Hoeltzli, S. D., and Frieden, C. (1996) *Biochemistry 35*, 16843−16851.
32. Hoeltzli, S. D., and Frieden, C. (1998) *Biochemistry 37*, 387−398.
33. Sacchettini, J. C., Scapin, G., Gopaul, D., and Gordon, J. I. (1992) *J. Biol. Chem. 267*, 23534−23545.
34. Koradi, R., Billeter, M., and Wuthrich, K. (1996) *J. Mol. Graphics 14*, 51−55.

BI0301688